Computed tomography of fossils and sulphide minerals from the Mesozoic of Turkey

Alexander Lukeneder[1], Susanne Lukeneder[1], Christian Gusenbauer[2]

[1]Geological and Palaeontological Department, Natural History Museum, Burgring 7, A-1010 Vienna, Austria, e-mail: alexander.lukeneder@nhm-wien.ac.at, susanne.lukeneder@nhm-wien.ac.at

[2]University of Applied Sciences Upper Austria, Wels Campus, Stelzhamerstrasse 23, 4600 Wels, Austria, e-mail: christian.gusenbauer@fh-wels.at

Abstract
We present a computed tomography and 3D visualisation of Mesozoic cephalopods from the Taurus Mountains. Study objects were single ammonoids and ammonoid mass-occurrences that were deposited during the Upper Triassic (approx. 234 mya) of SW Turkey. Computed tomography, a non-destructive and non-invasive method, facilitates the view inside rocks and fossils. The combination of computed tomography and palaeontological data enable us to produce 3D reconstructions of the extinct organism. Detailed reconstructions of the fossil cephalopods and the ammonoid animals are based on shell morphologies, adapted from CT data. Object-based combined analyses from computed tomography and various computed 3D facility programmes aid in understanding morphological details as well as their ontogenetic changes in fossil material. The presented CT data demonstrate the wide range of applications and analytical techniques, and furthermore outline possible limitations of computed tomography in earth sciences and palaeontology.

Keywords: computed tomography, ammonoids, iron sulphides, pyrite, marcasite, Triassic

1 Introducton

X-ray computed tomography and laser scanning is known in palaeontology as providing data for 3D visualisation and geometrical modelling techniques. Computed tomography and laser scans down to a few microns (or even below) of spatial resolution are increasingly employed for geoscientific investigations, using an equally variable range of processing techniques and software packages. Additionally, internal structures are visualised without the destruction of fossils, as computed tomography is a non-destructive method.

The creation of 3D models from fossils (e.g. cephalopods) based on CT aids in visualisation and interpretation, and may serve for the reconstruction of mechanical models. 3D models of fossil specimens have become increasingly popular, providing more or less accurate information about volume, spatial distribution, orientation and size of fossils in a sample as well as insights into biostratinomic and diagenetic processes. Numerous complementary techniques have been advanced in recent years. These provide 3D datasets of palaeontological objects and involve both surface and volume scanning methods (e.g. microtomography), as well as laser scanning (airborne, terrestrial or desktop scanners) of surface morphology. These methods can be combined with point cloud data generated from digital images. Numerous authors (e.g. [1-7]) show the multitude of applications of 3D geometrical models in palaeontological studies. The great variability, the wide range of applications, and the analytical techniques in the fossil record are demonstrated for dinosaurs [8-14], lizards [15], birds [16-18], fishes [19], mammals [20], molluscs [21-24], brachiopods [25], insects [26-28], plants [29-30, 23], algal or acritarch fossils [31], and protists [32-34]. The latter papers additionally outline possible limitations of 3D models in earth sciences and in palaeontology.

The main goal of this paper is to present methods and possibilities for visualisation of palaeontological material based on computed tomography, laser scanning and palaeontological features (e.g. morphology). Case studies on computed tomography within a 3-year project of the Austrian Science Fund (FWF P22109-B17) on Triassic ammonoids can demonstrate the increasing importance of CT and laser scanning methods in palaeontology.

2 Computed tomography

Non-invasive techniques, e.g. computed tomography, allow to process great volumes of information without causing any alteration of fossil material [22, 24]. The tomography scans used within this study were made at the Upper Austria University of Applied Science in Wels (Figure 1). The 3D computed tomography (CT) device RayScan 250 E is a 3D CT system equipped with two X-ray sources (a 225 kV micro-focus and a 450 kV mini-focus X-ray tube) for the inspection of a wide variety of parts, ranging from micro-objects (high resolution) to macroscopic ones (large penetration length). The system is additionally equipped with a 2048 x 2048 pixels flat-panel detector; it absorbs energy of the X-rays and re-emits the absorbed energy in the form of light, which can be detected. In the case of an industrial CT-system, the specimen is rotated by 360° and at each pre-defined angle step a 2D-projection image is captured. The complete set of projection images is then reconstructed to 3D volume data using a mathematical algorithm. The data consists of volumetric pixels (voxels), whose size limits the spatial resolution (down to 5µm) and the detail detectability. For each fossil part, the optimal voxel size and tube voltage were set according to the specimen's dimensions. A more detailed introduction to computed tomography is beyond the scope of this article. For the details of X-ray computed tomography as a technique of imaging and quantification of internal features of sediments and fossils see [35]. The non-destructive CT provides the basal information on morphological features of the respective fossil cephalopods.

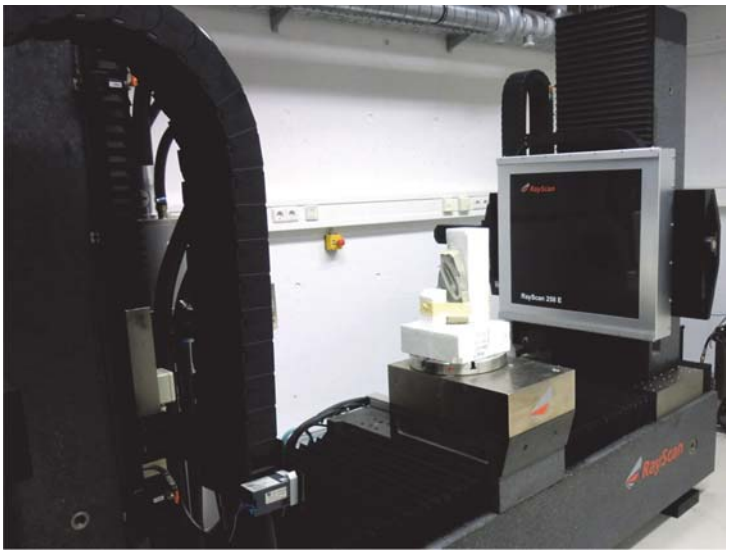

Figure 1: The CT RayScan 250 E device, with a 225 kV micro-focus and with a 450 kV mini-focus X-ray tube and a 2048 × 2048 pixel flat panel detector (cone beam reconstruction) located at the University of Applied Sciences Upper Austria, Wels Campus. Note the fixed limestone sample with the fossil in the centre.

3 Fossil material

Computed tomography was tested on the Triassic ammonoid genera Kasimlarceltites (and its mass-occurrence), Sandlingites and Trachysagentites (Figures 2, 3). These fossil cephalopods originate from the Upper Triassic (Carnian, approx. 234 mya) Aşağiyaylabel locality (Taurus Mountains, southwest Turkey). The material was collected within the FWF project P22109-B17 and is stored at the Natural History Museum in Vienna (NHMW). Inventory numbers are given for the investigated specimens of Kasimlarceltites (holotype NHMW-2012/0133/0014), Sandlingites (NHMW-2012/0133/0475) and Trachysagenites (NHMW-2012/0133/0350). The ammonoids were collected by Alexander and Susanne Lukeneder, Andreas Gindl, Mathias Harzhauser, Leopold Krystyn, Philipp Strauss, and Franz Topka.

The outcrop at Aşağiyaylabel is situated at steep limestone walls (dipping 50 degrees towards NE) within the Taurus Mountains of southern Turkey (Anatolia), about 90 km NNE of Antalya, between the lakes Egirdir and Beyşehir (GPS coordinates N37°33′05″ E31°18′14″; [36, 37]). The fossil cephalopods reported within this work derive from the Lower to Upper Carnian Kasimlar Formation (Julian 2–Tuvalian1, Austrotrachyceras austriacum Zone–Tropites dilleri Zone). A detailed description of the geology and lithostratigraphy is given in [36] and [37].

The investigated Upper Triassic ammonoids are Kasimlarceltites krystyni (family Celtitidae), Sandlingites cf. pilari (family Sandlingitidae) and Trachysagenites cf. beckei (family Haloritidae). All ammonoids are members of the order Ceratitida.

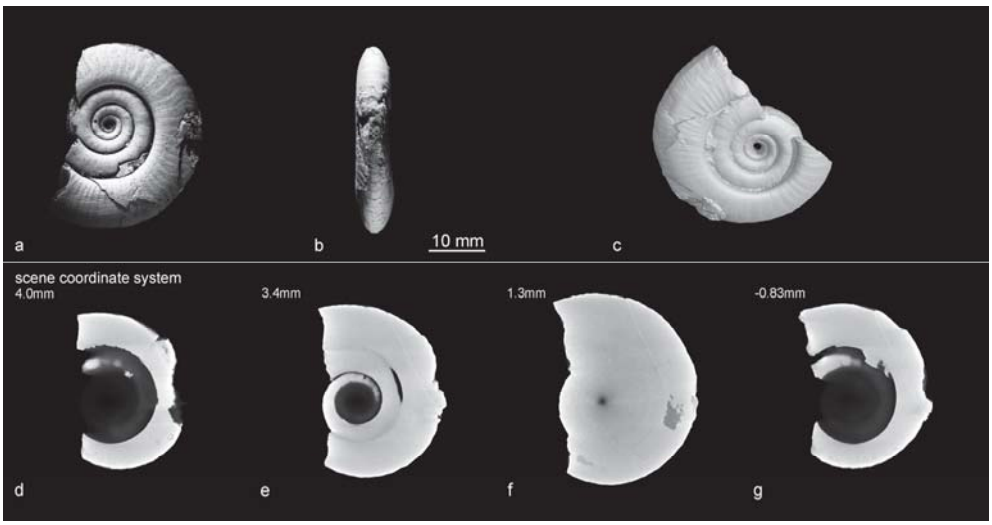

Figure 2: Computed tomography of a ceratitid ammonoid. *Kasimlarceltites krystyni*. a) Lateral view. b) ventral view of the holotype, NHMW-2012z0133/0014, both coated with ammonium chloride. c) rendered CT surface of the same specimen. CT frontal view slices. d) CT slice 048, e) CT slice 076. f) CT slice 168. g) CT slice 260. Embedding and infilling sediment is limestone. Performed on a RayScan 250 E device, with a 450 kV mini-focus X-ray tube and a 2048x2048 pixel flat panel detector (cone beam reconstruction). Slice spacing is 0.11 mm/pixel space. Specimen is 3.3 cm in diameter.

4 Results

3D computed tomography was performed with a 225 kV microfocus and a 450 kV minifocus X-ray tube. The specimens and the embedding fossiliferous marly limestone were tomographed frontally and axially (angle of 90°). Frontal and axial slice-images were animated to videos as motion pictures.
From the Triassic Kasimlarceltites (holotype, NHMW-2012/0133/0014; Figure 2) 320 frontal slices (0000.jpg-319.jpg; 146 MB) with 0.11 mm/pixel space were produced. The rock sample with the Kasimlarceltites mass-occurrence (NHMW-2013/0568/0003) appears with 310 frontal slices (000.jpg-309.jpg; 157 MB) with 0.11 mm/pixel space and 338 axial slices (527.jpg-864.jpg, 93.3 MB) with 0.11 mm/pixel space. From Sandlingites 463 frontal slices (000.jpg-462.jpg; 450 MB) with 0.11 mm/pixel space were produced. From Trachysagenites (Figure 3) 602 frontal slices (000.jpg-601.jpg; 388 MB) with 0.11 mm/pixel space were produced.
Measurements were performed with durations of 56, 68 and 92 minutes. Voxel sizes were 95 and 75.01 µm. Tube voltage was adjusted to 220 and 400 kV with 425 and 1500 µA. Exposure time was 600, 999, and 2000 ms. 1440 projections with a Cu pre-filter 1.0, 2.0 and 4.0 mm were made. Additionally, the surface (e.g. stone vs. air) was rendered to image the cephalopod's morphology.

The studies on computed tomography and laser scanning are essential for palaeontology and systematic investigations. Especially when extraction of fossils from embedding sediments is impossible, or the fossil and its delicate morphological parts (e.g. spines, ribs) would be destroyed by preparation.
Triassic ammonoid shells and filled phragmocones (both secondary calcite) from the Kasimlarceltites beds [37] possess the same mass-density as the matrix (i.e. limestone) in which the ammonoid specimens are embedded. The almost identical mass-density of the various carbonates of the embedding matrix (about 2.8 g/cm^3), the ammonoid shell (secondary calcite, about 2.6-2.8 g/cm^3), and the infilled matrix (about 2.8 g/cm^3) avoids their visualisation, especially of morphological details, via computed tomography. It is therefore not possible to visualise inner parts of the ammonoids by computed tomography. In few cases ammonoid shells, body chambers, and secondary formed calcite fissures can be observed in computed tomographic images and movies. For instance, a secondarily precipitated sparry calcite (in cleavage and cracks) is visible in the Triassic sample of the Kasimlarceltites beds. In contrast, hundreds of ammonoid specimens within that mass-occurrence "vanish" on CT slices. Disseminated pyrite cubes within the chambered part of the ammonoid (i.e. the phragmocone) define exactly the internal dimension and shape of Trachysagenites. Future work will be done within a project on the possibilities of computed tomography in such dense Mesozoic limestones. Two additional possibilities for using CT scans on material of similar density were described [28, 38]. The authors supposed to scan the material at low X-ray energy what reveals the different phases. By the use of a phase contrast holotomography at a synchrotron computed tomography device, crystal structures can be rendered visible [38].

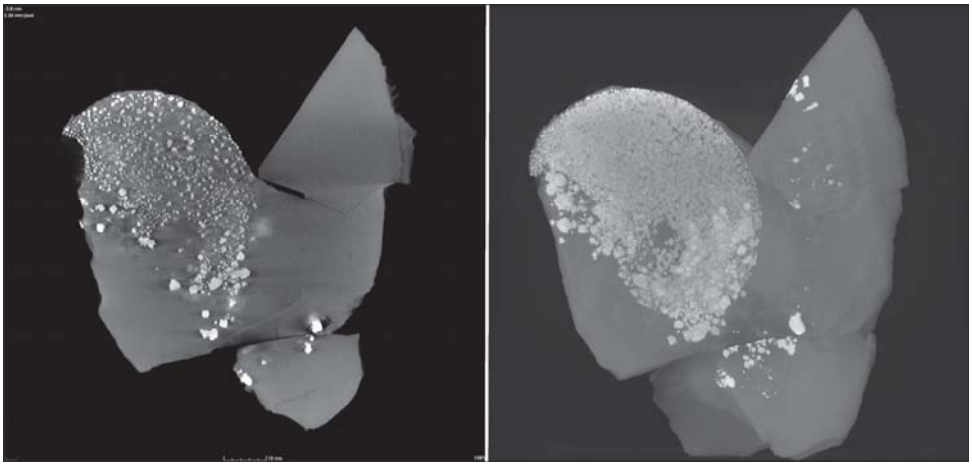

Figure 3: *Trachysagenites* cf. *beckei*. Lateral view, NHMW-2012/0133/0350. Embedding and infilling sediment is limestone. Note the numerous whitish pyrite cubes in the phragmocone. Computed tomography slice (left) and a maximum intensity projection (right) of the Triassic ceratitid ammonoid *T.* cf. *beckei*. Specimen is 12 cm in diameter.

5 Conclusions

The study presents results of an object-based combined analysis from computed tomography and various computed 3D facility programmes performed on the most complete shells of fossil cephalopods from Mesozoic sediments. Upper Triassic (Carnian) ammonoids from the Taurus Mountains in Turkey have been investigated.

The mentioned ammonoids are Kasimlarceltites krystyni, Sandlingites cf. pilari, and Trachysagenites cf. beckei. All of these are members of the order Ceratitida. The almost identical mass-density of the embedding limestone matrix (about 2.8 g/cm^3), the ammonite shell with secondary calcite (about 2.6-2.8 g/cm^3), and the infilled limestone matrix (about 2.8 g/cm^3) prevents the visualisation of internal parts and structures in the palaeontological material of the Upper Triassic from Turkey. Only pyrite cubes, formed in the phragmocone of a few ammonoids, passively show the morphology of the ammonoids' internal dimensions and structures (e.g. body chamber versus phragmocone).

In rare cases, the ammonoids are coated by iron sulphides as pyrite and marcasite (both FeS2) or by hydrated iron oxide-hydroxides as limonite (FeO(OH) × nH2O). Such steinkerns or limonitic fillings are detected by CT due to the increased density of these iron compounds (pyrite and marcasite: 4.8-5.0 g/cm^3; limonite: 2.7-4.3 g/cm^3). Dense structures as fine coatings on fossils or infillings of trace fossils can be visualised by computed tomography. Hence, pyritised or limonitic fossils bear the highest potential for high quality CT imaging and subsequent palaeontological reconstruction.

The use of computed tomography images and laser scans of fossil cephalopods from the Taurus Mountains of Turkey resulted in 3D visualisations. Moreover, computed tomography and palaeontological data were combined to produce 3D reconstructions, yielding animated clips running through CT data slices. The case studies demonstrate the non-destructive possibilities of 3D visualisation of palaeontological material. The resulting images are of high quality shots that are combined to short animated clips showing the morphology of fossils within CT slices in 3D. Another advantage is that the digital CT data, CT slices and CT clips can easily be shared amongst palaeontologists. This digital information can be discussed online and the resulting interpretation, based on the more detailed morphology, quickly adapted.

The additional use of high-speed 3D scans with reduced random-noise, obtained by efficient hyper-modulation, results in more detailed reconstructions by digitalisation of palaeontological material. Surfaces of ammonoids can therefore be reconstructed digitally without loss of information and digital-slices can be created from rendered outlines without any destruction of the fossil.

Acknowledgements

This study benefited from grants of the Austrian Science Fund (FWF) within the project P 22109-B17. The authors highly appreciate the help and support from the General Directorate of Mineral Research and Exploration (MTA, Turkey), and are thankful for the digging permission within the investigated area. Special thanks go to Yeşim İslamoğlu (MTA, Ankara) for organisation and guiding two field trips. We thank Alexander Rath (Vienna) for his advice with a software program to create movies of the 3D reconstructions and 3D laser scans. Macrophotographs of natural and coated ammonite specimens were taken by Alice Schumacher (Vienna).

References

[1] R. Marschallinger, Three-dimensional reconstruction and visualization of geological materials with IDL - examples and source code, Comp. & Geosci., 27 (4), 419-426, 2001.

[2] A.C. Maloof, C.V. Rose, R. Beach, B.M. Samuels, C.C. Calmet, D.H. Erwin, G.R. Poirier, N. Yao, F.J. Simons, Possible animal-body fossils in pre-Marinoan limestones from South Australia, Nature Geosci., 3, 653-659, 2010.

[3] S. Mayrhofer, A. Lukeneder, 3D Modellierung eines Karnischen Ammoniten Massenvorkommens (Taurus, Türkei; FWF P22109 B17). In: R. Marschallinger, W. Wanker, F. Zobl (Eds), Beiträge zur COGeo 2010, 12 pp., doi:10.5242/cogeo.2010.0000, 2010.

[4] I. Kruta, N. Landman, I. Rouget, F. Cecca, P. Tafforeau, The role of ammonites in the Mesozoic marine food web revealed by jaw preservation, Science, 331 (6013),70-72, 2011.

[5] R. Marschallinger, P. Hofmann, g. Daxner-Höck, R.A. Ketcham, Solid modeling of fossil small mammal teeth. Comp. & Geosci, 37 (9), 1364-1371,2011.

[6] S. Lukeneder, A. Lukeneder, Methods in 3D modelling of Triassic Ammonites from Turkey (Taurus, FWF P22109-B17), Proceedings IAMG 2011 Salzburg, 496-505, doi:10.5242/iamg.2011.0225, 2011.

[7] E.E. Saupe, R.P. Fuente, P.A. Selden, Delclos X., P. Tafforeau, C. Soriano, New Orchestina Simon, 1882 (Araneae: Oonopidae) from Cretaceous ambers of Spain and France: first spiders described using phase-contrast x-ray synchrotron microtomography, Palaeontology 55 (1), 127-143, 2012.

[8] E.J. Rayfield, D.B. Norman, C. Celeste, C.C. Horner, J.R. Horner, P.M. Smith, J. Jeffrey, J.J. Thomason, P. Upchurch Cranial design and function in a large theropod dinosaur. Nature, 409, 1033-1037, 2001.

[9] E.J. Rayfield, A.C. Milner, V.B. Xuan, P.G. Yound, Functional morphology of spinosaur 'crododile-mimic' dinosaurs, J. Vertebr. Paleontol. 27, 892-901, 2007.

[10] A.M. Balanoff, M.A. Norell, G. Grellet-Tinner, M.R. Lewin, Digital preparation of a probable neoceratopsian preserved within an egg, with comments on microstructural anatomy of ornithischian eggshells, Naturwissenschaften, 95, 493-500, 2008.

[11] L.M. Witmer, R.C. Ridgely, New insights into the brain, braincase and ear region of tyrannosaurs (Dinosauria, Theropoda), with implications for sensory organization and behavior, Anat. Rec., 292, 1266-1296, 2009.

[12] J. Fortuny, À. Galobart, C. de Santisteban, A new capitosaur from the Middle Triassic of Spain and the relationships within the Capitosauria, Acta Palaeontol. Polonica, 56 (3), 553-566, 2011.

[13] T. Tsuihiji, M. Watabe, K. Tsogtbaatar, T. Tsubamoto, R. Barsold, S. Suzuki, A.H. Lee, R. Ridgely, Y. Kawahara, L.M. Witmer, Cranial osteology of a juvenile specimen of Tarbosaurus bataar (Theropoda, Tyrannosauridae) from the Nemegt Formation (Upper Cretaceous) of Bugin Tsav, Mongolia, J. Vertebr. Paleontol., 31 (3), 497-517, 2011.
[14] F. Knoll, L.M. Witmer, F. Ortega, R.C. Ridgely, D. Schwarz-Wings, The braincase of the basal sauropod dinosaur Spinophorosaurus and 3D-reconstructions of the cranial endocast and inner ear, PLoS ONE 7 (1), e30060. doi:10.1371/journal.pone.0030060, 2012.
[15] M.J. Polcyn, J.V. Rogers, Y. Kobayashi, L.L. Jacobs, Computed tomography of an anolis lizard in Dominican amber: systematic, taphonomy, biogeography, and evolutionary implications, Palaeontol. Electr., 5 (1), 13 pp. http://palaeo-electronica.org/paleo/2002_1/amber/issue1_02.htm, 2002.
[16] T. Rowe, R.A. Ketcham, C. Denison, M. Colbert, X. Xu, P.J. Currie, Forensic palaeontology - the Archaeoraptor forgery, Nature, 410, 539-540, 2001.
[17] F.J. Degrange, C.P. Tambussi, K. Moreno, L.M. Witmer, S. Wroe, Mechanical analysis of feeding behavior in the extinct “terror bird” Andalgalornis steulleti (Gruiformes: Phorusrhacidae), PLoS ONE, 5 (8), e11856. doi:10.1371/journal.pone.0011856, 2010.
[18] D.K. Zelenitsky, F. Therrien, R.C. Ridgely, A.R. McGee, L.M. Witmer, Evolution of olfaction in non-avian dinosaurs and birds, Proc. R. Soc. B, Biol. Sci., 278, 3625-3634, 2011.
[19] Z. Gai, P.C.J. Donoghue, M. Zhu, P. Janvier, M. Stampanoni, Fossil jawless fish from China foreshadows early jawed vertebrate anatomy, Nature, 476, 324-327, 2011.
[20] Z.X. Luo, Z. Kielan-Jaworowska, R.L. Cifelli, In quest for a phylogeny of Mesozoic mammals, Acta Palaeontol. Polonica, 47, 1-78, 2002.
[21] R. Hoffmann, S. Zachow, Non-invasive approach to shed new light on the buoyancy business of chambered cephalopods (Mollusca), Proceedings IAMG 2011, Salzburg 2011, 507-517, 2011.
[22] A. Lukeneder, Computed 3D visualisation of an extinct cephalopod using computed tomographs, Comp. & Geosci., 45, 68-74, 2012.
[23] A. Lukeneder, S. Lukeneder, C. Gusenbauer, Computed tomography in palaeontology – case studies from Triassic to Cretaceous ammonites. In: EGU General Assembly 2012, 22-27 April, Vienna, Austria, Geophys. Res. Abstr., 14, 283, 2012.
[24] A. Lukeneder, S. Lukeneder, C. Gusenbauer, Computed tomography of fossils and sulphide minerals from the Mesozoic of Turkey, Conference on Industrial Computed Tomography ICT 2014, Wels, 2 pp., 2014.
[25] D. Gaspard, B. Putlitz, L. Baumgartner, X-ray computed tomography - apromising tool for brachiopod shell investigations, Proceedings IAMG 2011, Salzburg 2011, 518-533, 2011.
[26] R.J. Garwood, Palaeontology in the digital age. Part one: breathing new life into old bones, Mag. Geol. Ass., 9 (3), 18-20, 2010.
[27] R.J. Garwood, Palaeontology in the digital age. Part two: computerized Carboniferous creatures, Mag. Geol. Ass., 10 (2), 10-11, 2011.
[28] R.J. Garwood, J.A., Dunlop, M.D. Sutton, High-fidelity X-ray micro-tomography reconstruction of siderite-hosted Carboniferous arachnids, Biol. Lett., 5, 841-844, 2009.
[29] E.M. Friis, P.R. Crane, K.R. Pedersen, S. Bengtson, P.C.J., Donoghue, G.W. Grimm, M. Stampanoni, Phase-contrast X-ray microtomography links Cretaceous seeds with Gnetales and Bennettitales, Nature, 450, 549-552, 2007.
[30] A.C. Scott, J. Galtier, N.J. Gostling, S.Y. Smith, M.E. Collinson, M. Stampanoni, F. Marone, P.C.J. Donoghue, S. Bengtson Scanning electron microscopy and synchrotron radiation X-ray tomographic microscopy of 330 million year old charcoalfied seed fern fertile organs, Microsc. Microanal., 15, 166-173, 2009.
[31] J.A. Cunningham, C.W. Thomas, S. Bengtson, S.L. Kearns, S. Xiao, F. Marone, M. Stampanoni, P.C.J. Donoghue, Distinguishing geology from biology in the Ediacaran

Doushantuo biota relaxes constraints on the timing of the origin of bilaterians, Proc. R. Soc. B, Biol. Sci., 279, 2369-2376, 2012.
[32] P.C.J. Donoghue, S. Bengtson, X.P. Dong, N.J. Gostling, T. Huldtgren, J.A. Cunningham, C. Yin, Z. Yue, F. Peng, M. Stampanoni Synchrotron X-ray tomographic microscopy of fossil embryos, Nature, 442, 680-683, 2006.
[33] X.P. Dong, S. Bengtson, N.J. Gostling, J.A. Cunningham, T.H.P. Harvey, A. Kouchinsky, A.K. Val'kov, J.E. Repetsky, M. Stampanoni, F. Marone, P.C.J. Donoghue, The anatomy, taphonomy, taxonomy and systematic affinity of Markuelia: Early Cambrian to Early Ordovician scalidophorans, Palaeontology, 53 (6), 1291-1314, 2010.
[34] T. Huldtgren, J.A. Cunningham, C. Yin., M. Stampanoni, F. Marone, P.C.J. Donoghue, S. Bengtson, Fossilized nuclei and germination structures identify Ediacaran "animal embryos" as encysting protists, Science, 334, 1696-1699, 2011.
[35] F. Mees, R. Swennen, M. van Geet, P. Jacobs, Applications of X-ray computed tomography in the geosciences, Spec. Pap. Geol. Soc. London, 215, 1-243, 2003.
[36] S. Lukeneder, A. Lukeneder, M. Harzhauser, Y. Islamoglu, L. Krystyn, R. Lein, A delayed carbonate factory breakdown during the Tethyan-wide Carnian Pluvial Episode along the Cimmerian terranes (Taurus, Turkey), Facies, 58, 279-296, 2012.
[37] S. Lukeneder, A. Lukeneder, A new ammonoid fauna from the Carnian (Upper Triassic) Kasimlar Formation of the Taurus Mountains (Anatolia, Turkey), Palaeontology, doi:10.1111/pala.12070, 2014.
[38] R.J. Garwood, I.A. Rahman, M.D. Sutton, From clergymen to computers – the advent of virtual palaeontology, Geol. Today, 26 (3), 96-100, 2010.